Journal of Geodynamics 72 (2013) 59–66

Contents lists available at ScienceDirect

Journal of Geodynamics

journal homepage: http://www.elsevier.com/locate/jog

Estimate of glacial isostatic adjustment uplift rate in the Tibetan Plateau from GRACE and GIA models

T.Y. Zhang[a,b], S.G. Jin[a,*]

[a] Shanghai Astronomical Observatory, Chinese Academy of Sciences, Shanghai 200030, China
[b] University of Chinese Academy of Sciences, Beijing 100049, China

ARTICLE INFO

Article history:
Received 11 November 2012
Received in revised form 23 May 2013
Accepted 24 May 2013
Available online 2 June 2013

Keywords:
Glacial isostatic adjustment
GRACE
Tibetan Plateau

ABSTRACT

The Tibetan Plateau is located in central Asia with the highest mountain and extraordinary size, where geodynamic processes are very complex. The Glacial Isostatic Adjustment (GIA) effect in the Tibetan Plateau has been highly controversial because the past and present dimensions of ice sheets are suffering from large uncertainties. Larger differences in GIA estimates are found from different models or analyses based on the possible ice sheet and glacial history in Tibet. Present-day space geodetic techniques, such as Gravity Recovery and Climate Experiment (GRACE), are able to detect the vertical mass displacement and GIA uplift. In this paper, the GIA effects in the Tibetan Plateau are estimated and evaluated with GRACE measurements and GIA models. Four global GIA models and four regional models (RM) are respectively used to estimate the GIA uplift rates with various ice sheet models and viscoelastic Earth models, which are compared with GRACE measurements. Results show that the uplift rates of GIA effects range from 1 mm/yr to 2 mm/yr in the most part of the Tibetan Plateau. The global GIA model constructed by Peltier (Peltier, 2004) provides better estimations of the GIA in the Tibetan Plateau than the other three models.

1. Introduction

The Tibetan Plateau located in central Asia is subject to the northward push from the Indian subcontinent and the collision with Eurasian plate (e.g., Jin and Zhu, 2003; Jin and Park, 2006; Jin et al., 2007), which results in East-West expulsion and uplift (Fig. 1). The complex Tibetan Plateau called as the "Third Pole" attracts a lot of attention and different kinds of research due to its extreme size and elevation in the past. For the significant horizontal deformation, the GPS measurements have clearly revealed the main motion characteristics in Tibet (Wang et al., 2001). However, the larger uncertainties associated with the estimation of the vertical component using GPS measurements still create difficulties to determine accurately the vertical motion characteristics in the past time (Jin et al., 2005). Furthermore, the vertical motion and mechanism in Tibet is very complex. Several geodynamic processes control the complicated uplift pattern in the Tibetan Plateau, including the tectonic movement, glacier isostatic adjustment and the mass loss due to the climate change. Erkan et al. (2011) studied intensively and quantified the effect of these processes, which showed a significant and comparable difference to the geodetic observed signals. Recently, the uplift rates and crustal thickening rates were estimated using three stations of absolute gravimetry and three continuous GPS stations measurements, showing the mass loss in the Tibetan Plateau (Sun et al., 2009). However it is still difficult to determine the exact uplift rates due to the sparse continuous GPS sites and low resolution of the spatial distributed geodetic data.

In addition, the GIA, which is the Earth's viscoelastic response to the loading change from the glaciation and deglaciation during the glacial cycles, has big uncertainty in the Tibetan Plateau. In the past decades, it has always been very controversial whether there is a plateau-scale ice sheet as a key factor to assess the magnitude of GIA signal because of deficient precise estimates of the glaciations in Tibet. Larger differences in GIA estimates are found from different models or analyses on basis of the possible ice sheet and uncertain glacial history (Kaufmann and Lambeck, 1997; Kaufmann, 2005; Wang, 2001). They are mainly due to the input parameters limiting their forward modeling and the lack of actual and reliable observations. With the launch of the Gravity Recovery and Climate Experiment (GRACE) mission since 2002, it has been very successful to monitor the Earth's time-variable gravity field and to measure Earth's surface fluid mass redistribution (e.g., Jin et al., 2010), while GRACE also contains non-mass GIA effects. Therefore, the GRACE provides an opportunity to determine the mass balance and GIA effect in the Tibetan Plateau. In this paper the GIA uplift rates are estimated and evaluated from GRACE and other GIA models.

* Corresponding author.
E-mail addresses: zhangty@shao.ac.cn (T.Y. Zhang), gnss.jin@gmail.com (S.G. Jin).

0264-3707/$ – see front matter © 2013 Elsevier Ltd. All rights reserved.
http://dx.doi.org/10.1016/j.jog.2013.05.002

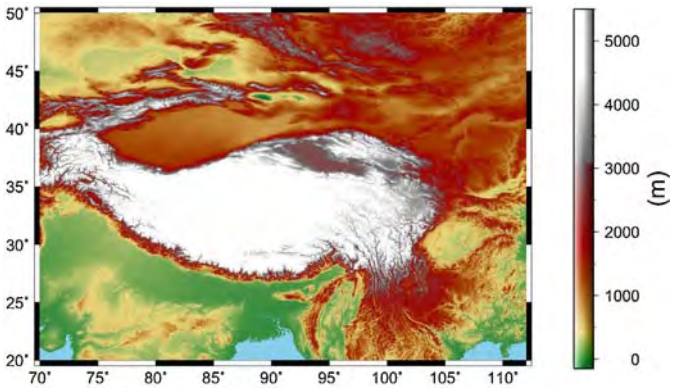

Fig. 1. The Tibetan Plateau and ice sheet model proposed by Kuhle et al. (1989).

2. Observations and results

2.1. Vertical displacements from GRACE

The Gravity Recovery and Climate Experiment (GRACE) mission with more than 10 year observations provides a unique opportunity to estimate global mass distribution within the Earth system (Tapley et al., 2004; Jin et al., 2011) and the vertical loading displacements, including the inseparable part of GIA signals. After excluding the loading displacements, i.e., mainly hydrological loading, the GIA uplift can be estimated from GRACE measurements. In this study, we use the monthly Stokes coefficients produced by the University of Texas Center for Space Research GRACE Release 04 (RL04) Level 2 to estimate the uplift mass displacement over the Tibetan Plateau with a post-processing, including de-correlation destriping, smoothing and filtering to reduce the dominated errors at high degrees (e.g., Swenson and Wahr, 2006; Chen et al., 2005; Wahr et al., 2004). The long-term variation of C_{30}, C_{40}, C_{21}, S_{21} components are added back in order to get the accurate trend of the surface mass displacement, and with regard to the less precise C_{20} component, it was replaced by the results from Satellite Laser Ranging data (Cheng and Tapley, 2004). Some missing monthly data are interpolated from the adjacent two month. The residual Stokes coefficients are obtained after removing the mean gravity field for 2003–2011. The mathematical relationships between the Stoke coefficients and radial surface displacements are expressed as follows (Wahr et al., 2000; Zhang et al., 2012):

$$dr_v(\theta,\lambda) = R\sum_{l=0}^{\infty}\sum_{m=0}^{l} W_l \frac{1+2l}{2}\tilde{P}_{lm}(\cos\ \theta)\cdot(\Delta C_{lm}(t)\cos\ m\lambda + \Delta S_{lm}(t)\sin\ m\lambda) \quad (1)$$

where $dr_v(\theta,\lambda)$ is the displacement in the radial direction, R is the radius of the Earth, $\tilde{P}_{lm}$ is the normalized Legendre function with degree of l and order of m, W_l is the Gaussian averaging kernel with a radius (here the radius of 500 km is used), and ΔC_{lm} and ΔS_{lm} are the residual Stokes coefficients of the mass.

2.2. Hydrologic loading displacements

Since the vertical mass displacements from GRACE are composed of several parts, including the hydrologic loads

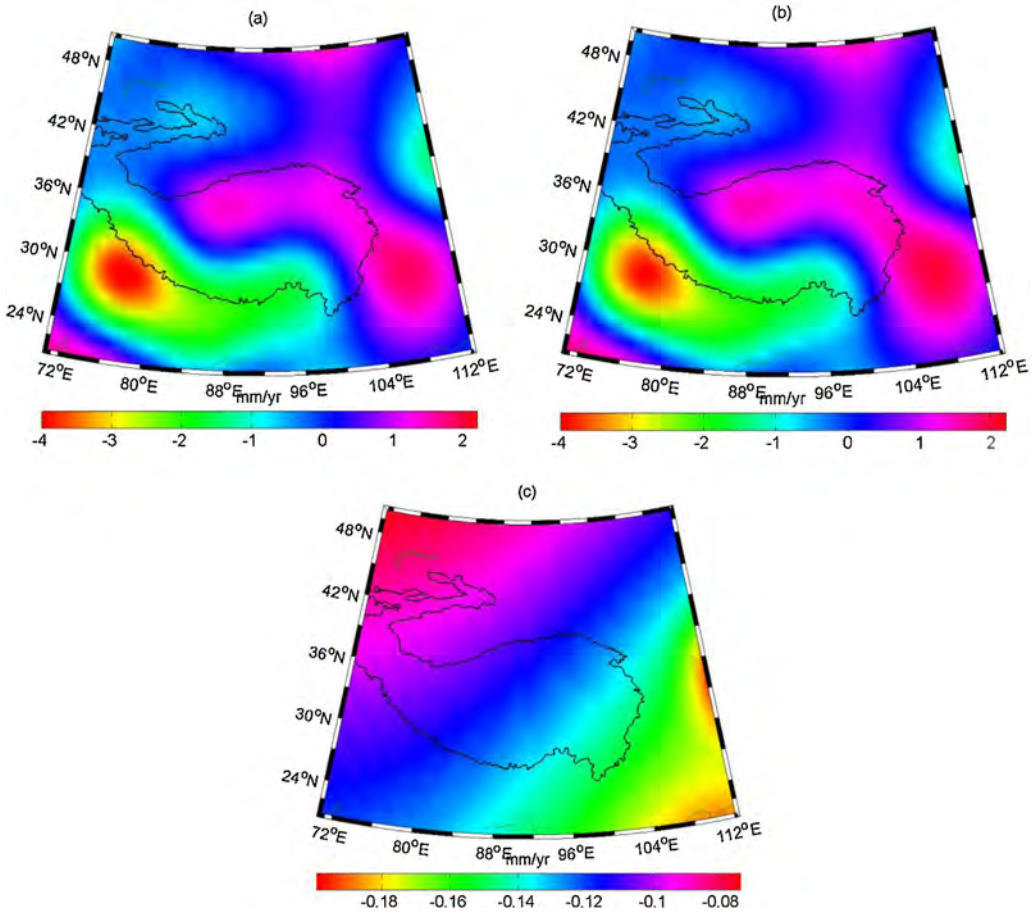

Fig. 2. (a) Uplift rates from GRACE in the Tibetan region including hydrological signals, (b) with removing the hydrological signals, and (c) the hydrological signals from WGHM.

(groundwater, soil moisture and glacier) and GIA, the stationary signal, including GIA, can be obtained when the hydrologic effects are removed (Tregoning et al., 2009). Some hydrologic models, like Global Land Data Assimilation System GLDAS and the WaterGAP Global Hydrology Model WGHM, are widely used to estimate the changes in total water storage, e.g., accumulated snow quantity and soil moisture. Because the hydrologic data in GLDAS are not available in the Tibet area, we could only use the WGHM model. The WGHM was developed for the assessment of the water resources situation, which describes well the global hydrological cycle (Döll et al., 1999; Alcamo et al., 2000). The hydrologic loading displacements in the Tibetan Plateau are estimated here using the distributed monthly water equivalent thickness of total water storage at each 1° spatial grid from the WGHM.

2.3. GIA estimate from GRACE in the Tibetan Plateau

The trend of vertical displacement is estimated from 10-year GRACE measurements based on Eq. (1). As a result, we can obtain some particular significant features through the linear rates and amplitude/phase of the annual periodic signals by least square estimates. After removing the secular hydrologic loading signals estimated from WGHM, the remaining trends are mainly dominated by the GIA. In order to strictly separate the viscoelastic effects of GIA from the hydrologic effects, the non-hydrologic Stokes spherical harmonic coefficients with truncation to degree 60 could be obtained by subtracting the monthly hydrological spherical harmonic coefficients estimated by the WGHM terrestrial water storage from the monthly GRACE results. Firstly the Stokes coefficients should be estimated from hydrologic WGHM model, which are then converted into the elastic components based on Eq. (2).

$$\begin{Bmatrix} \Delta\widehat{C}_{lm} \\ \Delta\widehat{S}_{lm} \end{Bmatrix} = \frac{\rho_{ave}(2l+1)}{3\rho_w(1+k_l)} \begin{Bmatrix} \Delta C_{lm} \\ \Delta S_{lm} \end{Bmatrix} \tag{2}$$

where $\Delta\widehat{C}_{lm}$ and $\Delta\widehat{S}_{lm}$ are the Stokes coefficients for the loading, ΔC_{lm} and ΔS_{lm} are the Stokes coefficients for geoid. ρ_{ave} is the average density of the earth, ρ_w is the density of the water, l is the order and k_l is the love number of order l. The hydrologic signals in Tibet captured by WGHM mainly reflect total terrestrial water mass change, and the remaining signals from GRACE are the

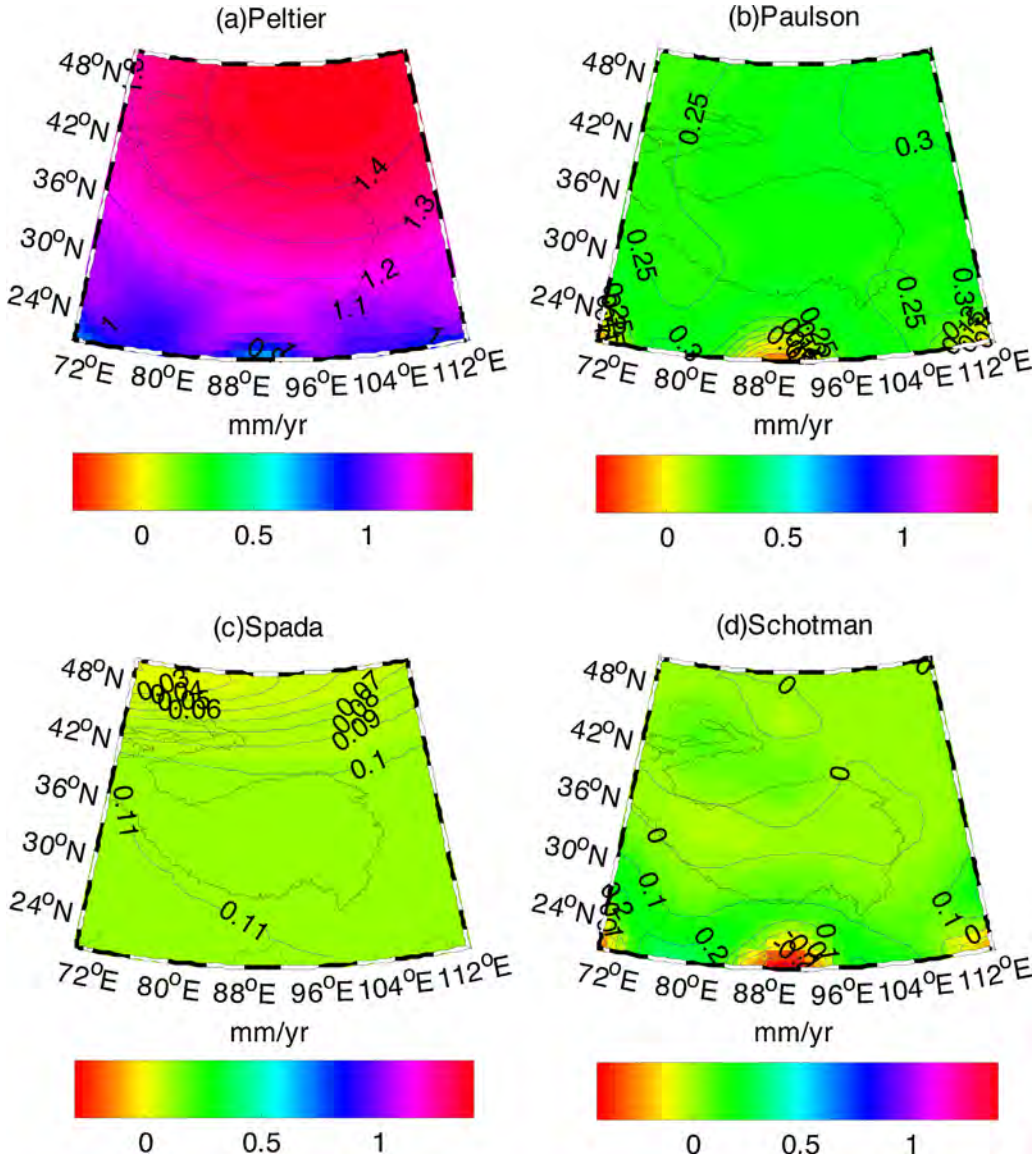

Fig. 3. Uplift rates from global GIA models constructed by (a) Peltier (Peltier, 2004), (b) Paulson (Paulson et al., 2007), (c) Spada (Spada et al., 2004), and (d) Schotman (Schotman et al., 2008).

Table 1
Parameters of the layered viscoelastic Earth models (Dziewonski and Anderson, 1981).

Model	layer	Radius (km)	Density (kg m^{-3})	Shear module (Pa)	Viscosity (Pa s)	
					A	B
Seven layers	0	3480–4220	1.093×104	0	0	0
	1	4220–4837	5.324×10^3	2.696×10^{11}	5.9×10^{21}	5.9×10^{21}
	2	4837–5331	4.993×10^3	2.32×10^{11}	5.9×10^{21}	5.9×10^{21}
	3	5331–5701	4.699×10^3	2.0×10^{11}	5.9×10^{21}	5.9×10^{21}
	4	5701–5971	4.474×10^3	1.734×10^{11}	5.9×10^{21}	5.9×10^{21}
	5	5971–6151	3.858×10^3	1.065×10^{11}	4.8×10^{20}	6.2×10^{20}
	6	6151–6256	3.476×10^3	7.649×10^{10}	4.8×10^{20}	6.2×10^{20}
	7	6256–6371	3.367×10^3	6.647×10^{10}	4.8×10^{20}	1.0×10^{19}

Model	Layer	Radius (km)	Density (kg m^{-3})	Shear module (Pa)	Viscosity (Pa s)
					C
Two layer	0	3480–5701	1.093×10^4	0	0
	1	5701–6256	4.919×10^3	2.17×10^{11}	5×10^{21}
	2	6256–6371	4.43×10^3	8.37×10^{10}	5×10^{20}

dominated viscoelastic deformation from GIA. Therefore we can get the trend from the monthly time series of radial displacement from the subtracted Stokes coefficients (Fig. 2).

3. GIA models and estimates

3.1. Ice model

The GIA models predict the uplift under the former ice load rebounds, but the magnitude and details of the effects predicted by GIA vary significantly between different models, mainly depending on the ICE-Sheet model and Earth structure model. As we can see from the models provided by Schotman and Spada (private contact) (Fig. 3), which are both based on the same Earth structure model but with different ICE-Sheet models, the general pattern of the radial velocity differs with each other and the signal of the vertical motion of both models are not consistent in the Tibetan plateau. In general, there are two types of ice models, respectively, such as global models ICE-3G, ICE-4G and ICE-5G, and regional models.

Two crucial unknown parameters deeply constrain the simulations of GIA in Tibet: the undetermined extent of ice sheet and the timing of glacial history. The spatial and temporal reconstructions of glaciers highly vary due to the lack of glacial geological data. An extreme example is the reconstruction done by Kuhle et al. (1989) where was assumed a plateau-scale ice sheet of the similar size as the Greenland ice sheet during the LGM (Last Glacial Maximum). This was based on the equilibrium line altitude reconstructions. Contrarily, Li et al. (1991) presented a map covering the whole area of the maximum Quaternary glacier extent where the plateau holds an ice sheet only about 20 percent of the area above 2000 m. This assumption was supported recently by other geological research and simulation of the growth and decay of the ice sheet in the Tibetan Plateau in response to the ensemble of climate forcing which come from Global Circulation Models (Kirchner et al., 2011). Owing to the lack of detailed description for Tibetan ice sheet when taking global ice sheet model as an idealized input to investigate the GIA effect in the Tibetan Plateau, it is not very convinced with regard to the unknown and diverse explanation of the icecaps during the LGM. As a result, it is necessary to take these two opposite ideas into account to model the GIA effects and evaluations. Here we take the thickness of the ice sheet as uniform and the glacial history as a saw function, assuming the values of 1000 m and 30 m referred to the results of the LGM, respectively.

3.2. Earth model

All the GIA models are composed of different ice sheet models and Earth rheological models where the Earth is divided into layers with different density and viscoelasticity values. We usually predict GIA on a spherically symmetric, compressible, Maxwell-viscoelastic, self-gravitating Earth model. The elastic and viscoelastic structures of our earth models are based on the Preliminary Reference Earth Model (PREM) (Dziewonski and Anderson, 1981), which is commonly used to represent the interior Earth of different rheological properties. The global ICE-3G, ICE-4G, ICE-5G were constructed by Peltier (1994, 1998b, 2004), which are coupled with different Earth models, such as VM1, VM2, under the constraint of the geodetic measurements. The variety of the viscoelasticity of stratified layers affects the calculation of the GIA. Therefore, it is extremely important to take it into account when selecting the proper Earth model. It should be emphasized that the medium between the core and mantle has been simplified by considering several homogenous layers. The normal structure of an Earth model is an elastic lithosphere as top layer with infinite viscoelasticity as top layer, a sub-lithospheric mantle which is taken as different viscoelastic layers with constant viscosity and an inviscid fluid and incorporated interior core. Some previous studies showed that it is reasonable and does not make large difference on the computation results (Vermeersen et al., 1996). Here we constructed three Earth models for regional GIA models with seven layers (A), seven layers (B) and two layers (C). (A) and (B) only differ on the viscosity parameters used. All the used viscoelastic parameters of the Earth model are listed in Table 1.

3.3. GIA models

There are some constructed GIA models for the prediction of the GIA signals in the whole solid Earth using the global ice sheet model (e.g., Paulson et al., 2007; Peltier, 2004). The four models shown in Fig. 3 for the Tibetean Plateau have been widely used for the correction and estimate of GIA in the radial rates. The four models are here named by first author, i.e., Peltier (Peltier, 2004), Paulson (Paulson et al., 2007), Spada (Spada et al., 2004), and Schotman (Schotman et al., 2008), and they are based on ICE-5G, ICE-5G, ICE-3G, modified ICE-3G ice sheet models, respectively. They show large differences in the spatial variation and magnitude between them, confirming the large uncertainties of the GIA models for Tibet. The selection of the Earth rheological model also influences the final model as observed when we compare the small magnitude of the GIA uplift in Paulson, Spada and Schotman models with the values given by the Peltier model.

Besides the four Global GIA models that fit the observables reasonably well at the area of prominent GIA signatures, like

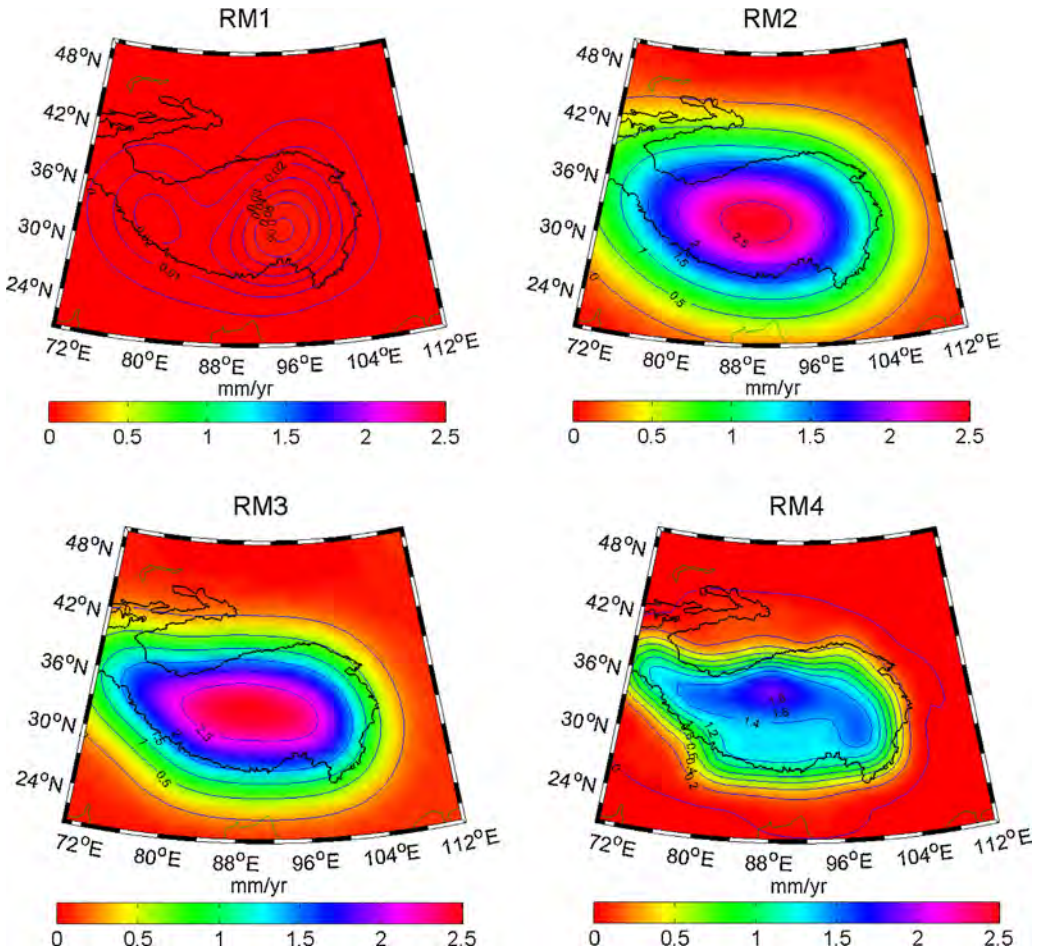

Fig. 4. Uplift rates in Tibet from four regional GIA models constructed by different ice models and Earth models (see Table 2).

North America and Fennoscandia, four regional models (RM) are further developed in this study. We focus on the comparison of the maximum estimates and the regional GIA effects in the central plateau. Here we use the ice models and Earth models mentioned in section 3.1 and section 3.2 to construct the four regional GIA models as detailed in Table 2.

Fig. 4 shows clearly that the RM1 model, based on ice sheet model by Li et al. (1991) predicts much smaller magnitudes of GIA rates when compared with the models based on the ice sheet model of Kuhle et al. (1989). Thus, we conclude that the glaciers of LGM in the Tibetan Plateau as proposed by Li do not contribute so much to the present uplift. The maximum glacier induced uplift appears in the central ice covered region. Both the magnitude and the region in the formerly glaciated area have a strong relation to the Earth model, while the model RM2, RM3 and RM4 show different uplift patterns. The maximum estimate of the uplift rates in model RM4 is smaller when compared to RM2and RM3 because a simpler two layered viscoelastic Earth model was applied.

Table 2
list of the regional models.

Model name	Ice model	Earth model
Regional Model 1(RM1)	Li (Li et al., 1991)	Seven layers-A
Regional Model 2(RM2)	Kuhle (Kuhle et al., 1989)	Seven layers-A
Regional Model 3(RM3)	Kuhle (Kuhle et al., 1989)	Seven layers-B
Regional Model 4(RM4)	Kuhle(Kuhle et al., 1989)	Two layers-C

4. Evaluation of GIA and discussion

In order to quantify the best fit between the models and the measurements, we minimized the misfit defined as

$$\chi^2 = \frac{1}{N}\sum_{i=1}^{N}\left(\frac{O_i - M_i}{\sigma_i}\right)^2 \quad (3)$$

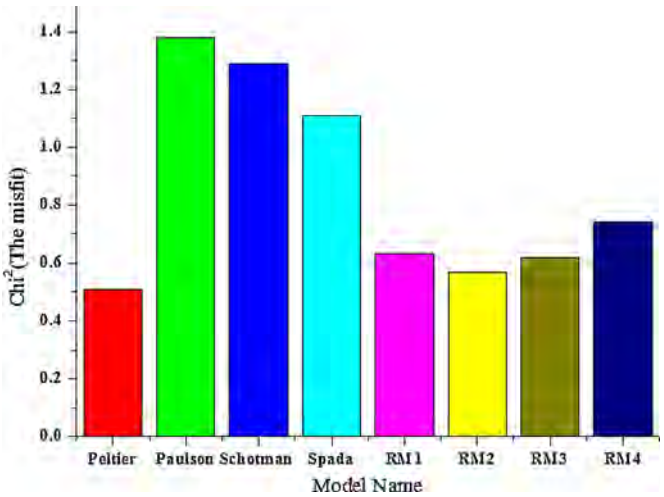

Fig. 5. The misfit χ^2 between GRACE and different models.

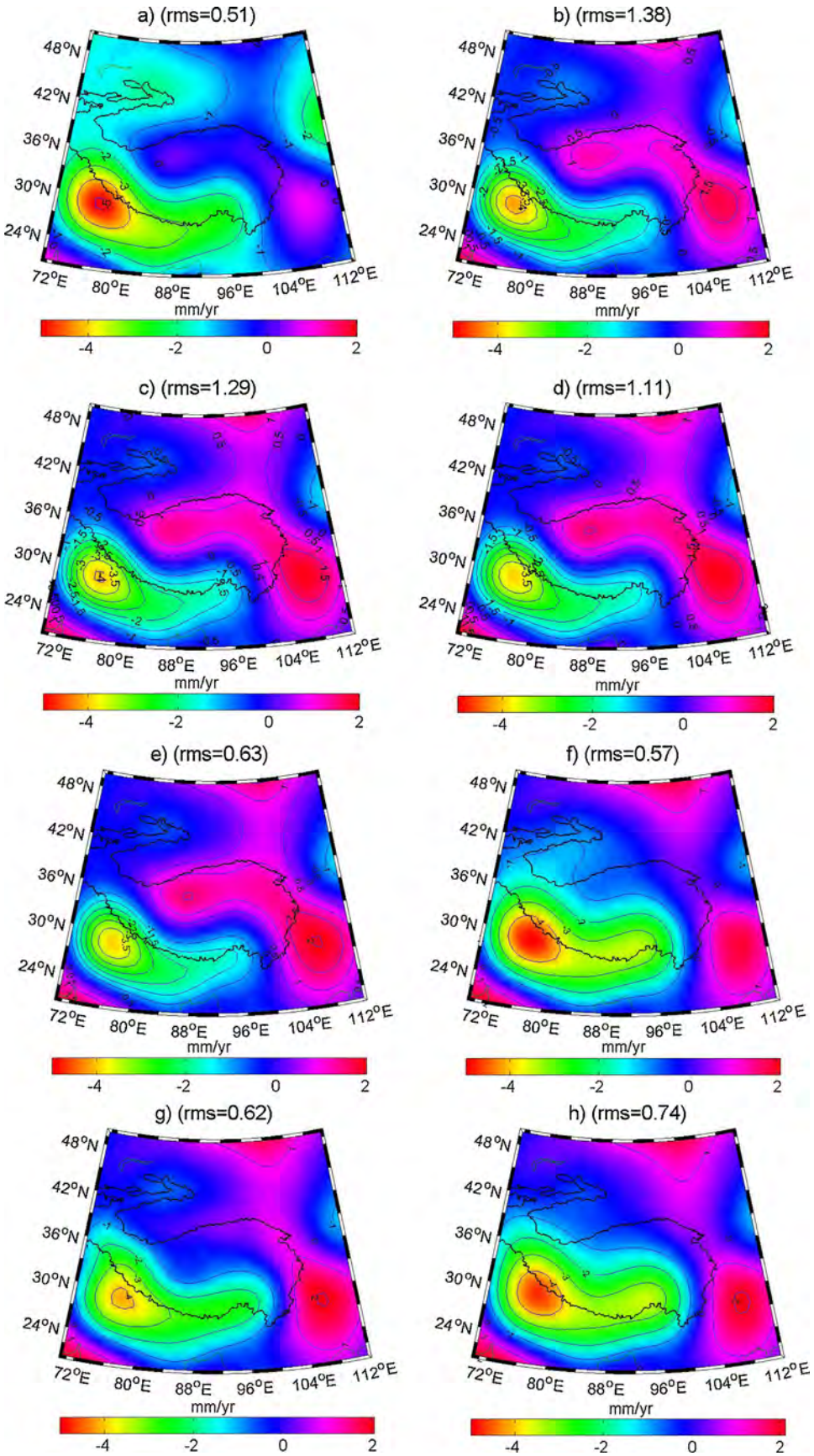

Fig. 6. Uplift rates from GRACE after the removal of hydrological signals and GIA effects from different models. The r.m.s. is calculated between GRACE without hydrological signals and the GIA models. (a) GRACE-WGHM-Peltier, (b) GRACE-WGHM-Paulson, (c) GRACE-WGHM-Spada, (d) GRACE-WGHM-Schotman, (e) GRACE-WGHM-RM1, (f) GRACE-WGHM-RM2, (g) GRACE-WGHM-RM3, and (h) GRACE-WGHM-RM4.

where N is the number of observations, O_i are the observations from GRACE measurements minus the hydrologiocal signal, M_i are from the GIA models corresponding to the GRACE grids and σ_i are the standard deviations of O_i. Many geophysical processes can affect the GRACE derived uplift rates, but many previous studies indict the capability of GRACE to detect the GIA signals (e.g., Tregoning et al., 2009; Purcell et al., 2011). By comparing directly with GRACE data, we investigate whether the GIA models show good agreement and they present similar spatial wavelength. To verify which model has better agreement with GRACE measurements, we calculate the misfit between them using Eq. (3).

All the GIA models do not show large consistency with the GRACE measurements (after the removal of hydrologic effects) as shown in Fig. 5. In order to investigate the potential GIA effects, we also subtract the linear trend given by the GIA models from the GRACE measurements. We can see clear which GIA model is the most compatible with GRACE minus total water storage with computing the misfit for the different models using a similar approach as given by Eq. (3). We should emphasize that the area in India are not taken into account because the WGHM did not model well the signal of the groundwater depletion in India (Rodell et al., 2009). The strong subsidence signal in Fig. 6 has not been well modeled, which could result in a bias of the comparison if such effect is not removed. Therefore, when we compare GIA models to GRACE results, we only consider inside of the Tibetan Plateau (delimited in Fig. 6 by the black line). Although the signal from the groundwater depletion in India may leak into the Tibetan Plateau, the Tibetan Plateau is far from the Northeast India and the effect is relatively small.

The comparison and analysis between the GRACE observations and the GIA models gives an initial estimate for GIA effects in the Tibetan Plateau. We can see that the most part of Tibetan Plateau has the GIA signal from 1 mm/yr to 2 mm/y and very small areas are close to 0 without obvious GIA effect. We conclude that the Peltier model shows the best agreement among the global models since it has the smallest r.m.s. (Fig. 5). Considering that all four global models are lacking real evidence and data in the area of Tibetan plateau, the uplift rates from the GIA model by Peltier may result from the effects of other areas, which need more research in the future. In addition, the regional model RM2 has the minimum r.m.s. when compared with the GRACE measurements (Fig. 5). In our regional GIA models, except for RM1, all the central areas are close to 2.5 mm/yr, which is a little larger than the GRACE observations shown in Fig. 2. The Northeast part of the Tibetan Plateau has values almost close to 2 mm/y, which is similar for all four models whereas the Southern part presents values close to 0 mm/yr, which may come from the leaked signal of groundwater depletion in India. The signal in the Western part of the Tibetan Plateau is also close to zero, which is similar to the ones modeled by our regional models because this area is not covered by ice sheet or only has very small ice sheet coverage. Therefore, GRACE measurements provide a chance to estimate the GIA effects in the Tibetan Plateau.

The uncertainty of GIA estimates from GRACE in Tibet is due mainly to the unmodeled mass loss from ice melting and groundwater in the hydrological model WHHM as well as GRACE measurements errors. On one hand, the WGHM may not accurately represent the total terrestrial water storage trend in Tibet, including the melted ice and groundwater, which will affect the GIA estimates. However, almost all melted ice goes to the lakes in Tibet, resulting in lake surface rise (Phan et al., 2012), while large-scale mass is almost balanced in the huge whole Tibetan system, indicating a smaller trend of ice mass loss in the whole Tibet. In addition, the groundwater depletion is smaller since Tibet has small populations and is also far from India. Therefore, the WGHM uncertainties should have no large effects on the trend estimates of ice-melting and groundwater in Tibet. On the other hand, the spatial resolution and accuracy of GRACE measurements can still affect the accuracy of the estimates of mass variations and GIA effects in Tibet. More satellite gravimetry data will allow us to obtain more accurate mass and GIA signals estimations in the future.

5. Conclusion

In this paper we have estimated and evaluated the GIA in the Tibetan Plateau using GRACE and different models. To estimate the GIA uplift rates, four commonly used global GIA models and four regional GIA models are used to investigate and evaluate the GIA. Our results are summarized as,

(1) The global model constructed by Peltier is better to estimate the GIA in the Tibetan Plateau than the other three global models. It is the best model to constrain the estimation of the GIA effects in the Tibetan Plateau.
(2) The GIA effects of the ice model proposed by Li et al. (1999) can be considered negligible due to small magnitude when compared to the observables. However, the GIA effects may be overestimated in central Tibetan Plateau when the ice model by Kuhle is used, depending on the viscosity of the Earth models. The viscosity of the asthenosphere makes a slightly difference in the computation of the uplift rates.
(3) The uplift rates of most part of the Tibetan Plateau range from 1 mm/yr to 2 mm/yr even if small parts in western part of the Tibetan Plateau show values close to 0 mm/yr. More precise data are needed to remove the effect of mass loss in order to further improve the GIA estimates in the Tibetan Plateau.
(4) The GRACE measurements may also improve the hydrological models and constrain the construction of more accurate ice sheet models. They provides a possible approach to constrain the ice sheet model in LGM because the ice model for the studies of GIA effects in Tibetan Plateau is of big uncertainty and the model proposed by Li and Kuhle neither can give convincible evidence.

Acknowledgements

The authors would like to thank those who made GRACE observations available. This work was supported by the National Keystone Basic Research Program (MOST 973) (Grant No. 2012CB72000), Main Direction Project of Chinese Academy of Sciences (Grant No.KJCX2-EW-T03), National Natural Science Foundation of China (NSFC) Project (Grant No. 11173050) and Shanghai Pujiang Talent Program Project (Grant No. 11PJ1411500).

References

Alcamo, J., Henrichs, T., Rösch, T., 2000. World Water in 2025 – Global modeling and scenario analysis for the World Commission on Water for the 21st Century Kassel World Water Series2. Center for Environmental Systems Research, University of Kassel, Germany http://www.usf.uni-kassel.de/usf/archiv/dokumente.en.htm

Cheng, M., Tapley, B.D., 2004. Variations in the earth's oblateness during the past 28 years. J. Geophys. Res. 109, B09402, http://dx.doi.org/10.1029/2004JB003028.

Chen, J.L., Wilson, C.R., Famiglietti, J.S., Rodell, M., 2005. Spatial sensitivity of GRACE time variable gravity observations. J. Geophys. Res. 110, B08408, http://dx.doi.org/10.1029/2004JB003536.

Dziewonski, A.M., Anderson, D.L., 1981. Preliminary reference earth model. Phys. Earth Planet. Int. 25, 297–356.

Döll, P., Kaspar, F., Alcamo, J., 1999. Computation of global water availability and water use at the scale of large drainage basins. Mathematische Geologie 4, 111–118.

Erkan, K., Shum, C.K., Wang, L., Guo, J., Jekeli, C., Lee, H., Panero, W.R., Duan, J., Huang, Z., Wang, H., 2011. Geodetic constraints on the Qinghai-Tibetan Plateau present-day geophysical processes. Terr. Atmos. Ocean. Sci. 22, 241–253, http://dx.doi.org/10.3319/TAO.2010.09.27.01.

Jin, S.G., Zhu, W., 2003. Active motion of tectonic blocks in eastern asia: evidence from GPS measurements. ACTA Geol. Sin. - Engl. Edn. 77 (1), 59–63, http://dx.doi.org/10.1111/j.1755-6724.2003.tb00110.x.

Jin, S.G., Wang, J., Park, P., 2005. An improvement of GPS height estimates: stochastic modeling. Earth Planets Space 57 (4), 253–259.
Jin, S.G., Park, P., 2006. Strain accumulation in South Korea inferred from GPS measurements. Earth Planets Space 58 (5), 529–534.
Jin, S.G., Park, P., Zhu, W., 2007. Micro-plate tectonics and kinematics in Northeast Asia inferred from a dense set of GPS observations. Earth Planet Sci. Lett. 257 (3–4), 486–496, http://dx.doi.org/10.1016/j.epsl.2007.03.011.
Jin, S.G., Chambers, D.P., Tapley, B.D., 2010. Hydrological and oceanic effects on polar motion from GRACE and models. J. Geophys. Res. 115, B02403, http://dx.doi.org/10.1029/2009JB006635.
Jin, S.G., Zhang, L., Tapley, B., 2011. The understanding of length-of-day variations from satellite gravity and laser ranging measurements. Geophys. J. Int. 184 (2), 651–660, http://dx.doi.org/10.1111/j.1365-246X.2010.04869.x.
Kaufmann, G., Lambeck, K., 1997. Implications of late pleistocene glaciation of the Tibetan Plateau for present-day uplift rates and gravity anomalies. Quat. Res. 48, 269–279.
Kaufmann, G., 2005. Geodetic signatures of a late pleistocene Tibetan ice sheet. J. Geodyn. 39, 111–125, http://dx.doi.org/10.1016/j.jog.2004.08.005.
Kirchner, N., Greve, R., Stroeven, A., Heyman, J., 2011. Paleoglaciological reconstructions for the Tibetan Plateau during the last glacial cycle: evaluating numerical ice sheet simulations driven by GCM-ensembles Quat. Sci. Rev. 30 (2011), 248–267.
Kuhle, M., Herterich, K., Calov, R., 1989. On the ice age glaciation of the Tibetan Highlands and its transformation into a 3D model. Geogr. J. 19 (2), 201–206.
Li, B., Li, J., Cui, Z., 1991. Quaternary Glacial Distribution Map of Qinghai Xizang (Tibet) Plateau 1:3,000 000 Lanzhou University.
Paulson, A., Zhong, S., Wahr, J., 2007. Inference of mantle viscosity from GRACE and relative sea level data. Geophys. J. Int. 171 (2), 497–508.
Peltier, W.R., 1994. Ice age paleotopography. Science 265, 195–201.
Peltier, W.R., 1998b. A space geodetic target for mantle viscosity discrimination: Horizontal motions induced by glacial isostatic adjustment. Geophys. Res. Lett. 25, 543–546.
Peltier, W.R., 2004. Global glacial isostasy and the surface of the ice-age earth: The ICE-5G (VM2) model. Annu. Rev. Earth Planet. Sci. 32, 111–149.
Phan, V.H., Lindenbergh, R., Menenti, M., 2012. ICESat derived elevation changes of Tibetan lakes between 2003 and 2009. Int. J. Appl. Earth Obs. Geoinform. 17, 12–22.
Purcell, A., Dehecq, A., Tregoning, P., Potter, E.-K., McClusky, S.C., Lambeck, K., 2011. Relationship between glacial isostatic adjustment and gravity perturbations observed by GRACE. Geophys. Res. Lett. 38, L18305, http://dx.doi.org/10.1029/2011GL048624.
Rodell, M., Velicogna, I., Famiglietti, J.S., 2009. Satellite-based estimates of groundwater depletion in India. Nature 460, 999–1002.
Schotman, H.H.A., Wu, P., Vermeersen, L.L.A., 2008. Regional perturbations in a global background model of glacial isostasy. Phys. Earth Planet. Inter. 171, 323–335.
Spada, G., Antonioli, A., Boschi, L., Cianetti, S., Galvani, G., Giunchi, C., Perniola, B., Piana Agostinetti, N., Piersanti, A., Stocchi, P., 2004. Modeling Earth's postglacial rebound, EOS. Trans. Am. Geophys. Union 85, 62–64.
Sun, W., Wang, Q., Li, H., Wang, Y., Okubo, S., Shao, D., Liu, D., Fu, G., 2009. Gravity and GPS measurements reveal mass loss beneath the Tibetan Plateau: Geodetic evidence of increasing crustal thickness. Geophys. Res. Lett. 36, L02303, http://dx.doi.org/10.1029/2008GL036512.
Swenson, S.C., Wahr, J., 2006. Post-processing removal of correlated errors in GRACE data. Geophys. Res. Lett. 33, L08402, http://dx.doi.org/10.1029/2005GL025285.
Tapley, B.D., Bettadpur, S., Ries, J.C., Thompson, P.F., Watkins, M.M., 2004. GRACE measurements of mass variability in the earth system. Science 305, 503–505, http://dx.doi.org/10.1126/science.1099192.
Tregoning, P., Ramillien, G., McQueen, H., Zwartz, D., 2009. Glacial isostatic adjustment and nonstationary signals observed by GRACE. J. Geophys. Res. 114, B06406, http://dx.doi.org/10.1029/2008JB006161.
Vermeersen, L., Sabadini, R., Spada, G., 1996. Analytical visco-elastic relaxation models. Geophys. Res. Lett. 23, 697–700.
Wahr, J., Wingham, D., Bentley, C., 2000. A method of combining ICESat and GRACE satellite data to constrain Antarctic mass balance. J. Geophys. Res. 105 (B7), 6279–16294.
Wahr, J., Swenson, S., Zlotnicki, V., Velicogna, I., 2004. Time-variable gravity from GRACE: First results. Geophys. Res. Lett. 31, L11501, http://dx.doi.org/10.1029/2004GL019779.
Wang, H., 2001. Effects of glacial isostatic adjustment since the late Pleistocene on the uplift of the Tibetan Plateau. Geophys. J. Int. 144, 448–458, http://dx.doi.org/10.1046/j.1365-246x.2001.00340.x.
Wang, Q., Zhang, P.Z., Freymueller, J.T., Bilham, R., Larson, K.M., Lai, X., You, X., Niu, Z., Wu, J., Li, Y., Liu, J., Yang, Z., Chen, Q., 2001. Present-day crustal deformation in China constrained by Global Positioning System measurements. Science 294, 574–577, http://dx.doi.org/10.1126/science.1063647.
Zhang, L.J., Jin, S.G., Zhang, T.Y., 2012. Seasonal variations of Earth's surface loading deformation estimated from GPS and satellite gravimetry. J. Geod. Geodyn. 32 (2), 32–38.